Scientific Reports

https://doi.org/10.1038/s41598-026-43201-8

Article in Press

Synergistically micronutrient co-application improves nutritional quality and effectively reduces aflatoxin contamination in *Brassica rapa* L. roots

Received: 3 January 2026

Accepted: 2 March 2026

Published online: 08 March 2026

Cite this article as: Siraj U., Siraj Z. & Ríos-Escalante P.R. Synergistically micronutrient co-application improves nutritional quality and effectively reduces aflatoxin contamination in *Brassica rapa* L. roots. *Sci Rep* (2026). https://doi.org/10.1038/s41598-026-43201-8

Unays Siraj, Zainab Siraj & Patricio R. Ríos-Escalante

Synergistically Micronutrient Co-application Improves Nutritional Quality and Effectively Reduces Aflatoxin Contamination in *Brassica rapa* L. Roots.

Unays Siraj [A B *], **Zainab Siraj** [C], **Patricio R. De Lo Ríos-Escalante** [D E]

[A] Department of Biotechnology, Faculty of Science, Mahidol University, Bangkok, 10400, Thailand.
[B] Department of Zoology, Faculty of Life Sciences, Abdul Wali Khan University, Mardan 2300, Pakistan. **ORCID** - https://orcid.org/0000-0002-8686-0540
[C] Department of Human Nutrition and Dietetics, Women's University, Mardan, 23200, Pakistan - **Email.** Zk0983998@gmail.com
[D] Departamento de Ciencias Biologicas Químicas, Facultad de Recursos Naturales, Universidad Católica de Temuco Casila 15-D Temuco, Chile
[E] Núcleo de Estudios Ambientales, Faculted de Recursos Naturales, Universidad Catolica de Temuco. **ORCID.** https://orcid.org/0000-0001-5056-7003. **Email**. prios@uct.cl

* **Corresponding author.** Unays Siraj - **Email.** unayskhan@gmail.com

Abstract. Aflatoxin B1 (AFB_1) contamination and micronutrient deficiencies pose a major challenge to food safety and nutritional security. This study elucidated the synergistic potential of boron (B) and zinc (Zn) co-application to fortify nutritional quality and mitigate AFB_1 accumulation in turnip (*Brassica rapa* L) roots. Seeds were cultivated in soils amended with individual or combined B and Zn at concentrations of 10-25 mg kg^{-1}. In results, individual B supplementation at 20 mg kg^{-1} optimized protein content (10.9%), and the B-Zn interactome provided superior overall metabolic performance. B-Zn synergy significantly enhanced physiological resilience. Specifically, the combined application at 15-20 mg kg^{-1} consistently achieved the highest STI and GMP productivity across biochemical traits. Carbohydrate partitioning was significantly improved, with NFE reaching 74.1% at 20 mg kg^{-1} of B + Zn. AFB_1 toxicity was suppressed by 60.08% at 15 mg kg^{-1}. RPI of dry matter, protein, and phenolic were consistently positive at 15-20 mg kg^{-1} of B + Zn. Co-application enhanced the YSI for NFE, protein, and ash content. PCA confirmed that the synergistic effects of B + Zn treatment provided superior nutritional results compared to individual micronutrient applications. These findings demonstrate that balanced B-Zn supplementation strengthens nutritional composition quality and suppresses AFB_1 contamination, supporting the biofortification paradigm as a reproducible strategy for sustainable food quality and crop improvement.

Keywords: Proximate composition, Nutritional value, Food quality, Phenolic compounds, Antioxidant activity, Stress tolerance

Introduction. Food contamination by mycotoxins (MTs) and heavy metal toxicity presents a major global food challenge. Toxic heavy metals weaken plant defenses through oxidative stress, creating favorable conditions for *Aspergillus* proliferation and toxin production. The fungus produces MTs to chelate metal ions, reducing their mobility and toxicity [1]. The double-edged response enabled fungal survival in a contaminated environment, simultaneously increasing the risk of food contamination. MTs are secondary metabolites produced during crop growth, storage, and distribution, stimulated as a mechanism of resistance [2]. Among them, aflatoxin B_1 (AFB_1) is the most potent and hazardous MT, strongly linked to hepatocellular carcinoma (HCC) [3]. Its ingestion triggers immune suppression, teratogenesis, and neurological impairment [4]. AFB_1 exhibits clinical synergy with Hepatitis B (HBV) or Hepatitis C (HCV) infections [5], significantly compounding health risks. Its toxicity is estimated to be 68 times greater than arsenic, showing an extreme risk to human health. AFB_1 contaminates nearly one-quarter of the global food supply [6]. According to the WHO/FAO Codex Alimentarius 2025 [7], AFB_1 poses a major global health and food safety threat, particularly in developing regions reliant on subsistence farming.

AFB_1 exerts its toxicity through oxidative stress, lipid peroxidation, and genotoxicity, processes modulated by antioxidant enzymes such as superoxide dismutase (*SOD*) and catalase (*CAT*) [8]. Its chemical stability even under thermal and chemical treatment complicates detoxification [9]. Consequently, strategies that improve nutritional resilience while suppressing toxin accumulation are urgently needed.

Proximate analysis, including protein, fiber, ash, moisture, fat, and phenolic, provides a direct measure of nutritional value, food quality, and industrial applicability of crops. Thereby linking biochemical composition to food safety and consumer health. Micronutrients such as boron (B) and zinc (Zn) are central to these traits. Zn is pivotal for enzyme activation, pathogen defense, and maintaining membrane integrity [10]. Zn uptake is mediated by Zinc-regulated transporter (ZIP), which transports divalent metals into the cytosol [11], and Natural Resistance-associated Macrophage Protein transporters (NRAMP), which redistribute ions across the membrane to maintain homeostasis [12]. Zn-enriched biofertilizers have been reported to enhance phenolic biosynthesis, crop yield, and mitigate symptoms of biotic and abiotic stress [13] [14]. B uptake relies on high boron-requiring efflux transporters (BOR) and nodulin -26-like intrinsic protein (NIP) channels, which together stabilize the membrane and confer stress tolerance [15]. Beyond transport, B regulates meristem activity, gene expression, and plays essential roles in carbohydrate metabolism, lignin biosynthesis, and cell wall development [16]. The combined supplementation of B and Zn has been shown to support key metabolic processes and modulate antioxidant responses in crops [17].

Previous studies highlighted the individual and combined roles of B and Zn in mitigating stress and improving *Brassica rapa* L quality. In addition, a moderate level of B + Zn is associated with enhanced proline and protein [17]. *B. rapa* L. is widely cultivated for its edible roots, valued for their rich nutritional profile and medicinal properties [18]. The push for climate-resilient agriculture has intensified interest in micronutrient-based interventions as sustainable alternatives [17]. Due to the excessive use of fertilizer, environmental pollution has degraded soil quality and microbial biodiversity, increasing interest in biofertilizer-based remediation strategies [19]. However, oversupply of micronutrients can induce toxicity. Zn in elevated concentrations triggers Cd-like toxicity symptoms, such as growth inhibition and impaired photosynthesis efficiency. Similarly, excessive B disrupts protein synthesis, cell division, and differentiation [20].

We hypothesized that the co-application of B and Zn would exert a synergistic effect on the nutritional composition and reduce AFB_1 in *B. rapa* L roots. This treatment is expected to enhance proximate composition and improve food safety by limiting AFB_1 accumulation. Our study also aimed to evaluate the optimal concentration range for synergistic interaction. B and Zn were selected for their established roles in antioxidant defense, cell integrity, and enzyme activity. Thus, we tested whether the combined application could more effectively improve proximate composition and mitigate AFB_1 contamination compared with individual treatments.

Results

Effect of treatment on NFE content. The application of B and Zn treatments significantly influenced the NFE content in *B. rapa* L. roots, with responses being highly concentration dependent. The simultaneous application of B and Zn at 15 and 20 mg kg^{-1} resulted in a 10.2% and 11.2% increase in NFE, compared with the untreated control (66.6% ± 0.1). The combined B + Zn application at 20 mg kg^{-1} yielded the maximum NFE value of (74.1% ± 0.25). However, post-hoc analysis indicates that this performance is statistically comparable to the 25 mg kg^{-1} treatment cohort (70.8% ± 0.2, $p > 0.05$). A saturation followed by a decline in metabolic enhancement within the 20 and 25 mg kg^{-1} treatments. Further, equates to this corresponds to a 3.6% and 2.2% enhancement relative to the individual B (71.5%) and Zn (72.5%) applications at equivalent dosages, respectively (**Table 1)**.

Table 1. Nitrogen-free extract (NFE) content of *B. rapa* L. roots cultivated under B, Zn, and combined B + Zn treatments at concentrations of 10, 15, 20, and 25 mg kg^{-1}.

Groups	Control	10 mg kg^{-1}	15 mg kg^{-1}	20 mg kg^{-1}	25 mg kg^{-1}
Boron	66.6 ± 0.1^{a}	71.9 ± 1.4^{b}	69.9 ± 1.4^{ab}	71.5 ± 0.5^{b}	72.8 ± 0.7^{b}
Zinc		72.6 ± 0.6^{b}	69.3 ± 0.2^{ab}	72.5 ± 0.2^{b}	72.2 ± 0.3^{b}
Boron + Zinc		68.6 ±0.3^{ab}	73.4 ± 0.1^{b}	74.1 ± 0.25^{b}	70.8 ± 0.2^{ab}

Values are presented as mean ± SD from three independent replicates (*n=3*). Superscript letters indicate significant differences at $p < 0.05$ according to one-way ANOVA followed by Tukey's post hoc test. All values are expressed on a fresh weight (FW) basis.

Effect of treatment on Dry matter content. Combined B + Zn supplementation at 25 mg kg^{-1} elicited a statistically significant enhancement in dry matter content (91.1% ± 0.02), showing an 0.8% increase relative to the untreated control (90.3% ± 0.1; **Table 2**). This marginal gain was significant only at the highest co-application level (25 mg kg^{-1}), showing a threshold effect rather than a gradual concentration-dependent trend. Further, lower co-application levels (10 -20 mg kg^{-1}) did not surpass the efficacy of individual nutrient treatments, remaining statistically similar to the control.

Table 2. Dry matter content of *B. rapa* L. roots cultivated under B, Zn, and combined B + Zn treatments at concentrations of 10, 15, 20, and 25 mg kg^{-1}.

Groups	Control	10 mg kg^{-1}	15 mg kg^{-1}	20 mg kg^{-1}	25 mg kg^{-1}
Boron	90.3 ± 0.1^{a}	90.6 ± 0.01^{a}	90.5 ± 0.02^{a}	90.7 ± 0.02^{a}	90.6 ± 0.02^{a}
Zinc		90.4 ± 0.02^{a}	90.6 ± 0.01^{a}	90.3 ± 0.02^{a}	90.2 ± 0.03^{a}
Boron + Zinc		90.4 ± 0.15^{a}	90.0 ± 0.01^{a}	89.7 ± 0.01^{a}	91.1 ± 0.02^{b}

Values are presented as mean ± SD from three independent replicates (*n=3*). Different superscript letters indicate significant differences at $p < 0.05$ according to one-way ANOVA followed by Tukey's post hoc test. All values are expressed on a fresh weight (FW) basis.

Effect of treatment on moisture content. It is imperative to identify the optimal concentration and combination of these nutrients that may enhance plant energy storage and overall crop performance. In this study, moisture content varied significantly across different concentrations of B and Zn applied. The control group exhibited the highest moisture content (9.8%; **Table 3**), whereas the group treated with the 10 mg kg^{-1} of B + Zn displayed slightly lower values of 9.6%. Although moisture content was lower at 10 mg kg^{-1}, statistically significant differences were observed among B, Zn, and B + Zn treatments. Zn supplementation at 15 mg kg^{-1} resulted in 9.4%, which was a lower moisture content compared with B alone (9.5%). Conversely, the combination of B + Zn yielded a significantly higher moisture at 20 mg kg^{-1} (10.3%) compared with all individual treatments. However, at 25 mg kg^{-1}, moisture content declined sharply to 8.9%, showing that excessive co-application induces stress and disrupts water retention capacity. Thereby marking 20 mg kg^{-1} as the optimal threshold for moisture enhancement.

Table 3. Moisture content of *B. rapa* L. roots cultivated under B, Zn, and combined B + Zn treatments at concentrations of 10, 15, 20, and 25 mg kg^{-1}.

Groups	Control	10 mg kg^{-1}	15 mg kg^{-1}	20 mg kg^{-1}	25 mg kg^{-1}
Boron	9.8 ± 0.1 ^{a}	9.4 ± 0.1 ^{a}	9.5 ± 0.2 ^{a}	9.2 ± 0.2 ^{a}	9.4 ± 0.1 ^{a}
Zinc		9.6 ± 0.1 ^{a}	9.4 ± 0.1 ^{a}	9.7 ± 0.1 ^{a}	9.8 ± 0.2 ^{a}
Boron + Zinc		9.6 ± 0.1 ^{a}	10.0 ± 0.1 ^{ab}	10.3 ± 0.1 ^{b}	8.9 ± 0.1 ^{c}

Values are presented as mean ± SD from three independent replicates ($n=3$). Different superscript letters indicate significant differences at $p < 0.05$ according to one-way ANOVA followed by Tukey's post hoc test. All values are expressed on a fresh weight (FW) basis.

Effect of treatment on protein content. Protein values ranged from 7.9-10.9.9% crude protein, with significant difference among groups ($p < 0.05$; **Table 4**). The control group exhibited the highest protein content (10.1 %), while the lowest was observed under co-application of 15 mg kg^{-1} of B + Zn (7.9 %), showing a 21.8% reduction relative to the control. In contrast, individual B supplementation at 20 mg kg^{-1} increased the peak protein content (10.9%). Among the combined treatments, a higher concentration of B + Zn (20-25 mg kg^{-1}) increased protein levels to a maximum of (9.1%), reflecting 15% improvement over the 15 mg kg^{-1} co-application.

Table 4. Protein content of *B. rapa* L. roots cultivated under B, Zn, and combined B + Zn treatments at concentrations of 10, 15, 20, and 25 mg kg^{-1}.

Groups	Control	10 mg kg^{-1}	15 mg kg^{-1}	20 mg kg^{-1}	25 mg kg^{-1}
Boron	10 ± 0.1 ^{ab}	9.9 ± 0.2 ^{ab}	9.0 ± 0.2 ^{bc}	10.9 ± 0.1 ^{a}	8.6 ± 0.2 ^{c}
Zinc		10.3 ± 0.1 ^{a}	9.9 ± 0.2 ^{ab}	10.7 ± 0.1 ^{a}	10.0 ± 0.2 ^{ab}
Boron + Zinc		10.3 ± 0.2 ^{ab}	7.9 ± 0.1 ^{c}	10.0 ± 0.2 ^{ab}	9.1 ± 0.2 ^{bc}

Values are presented as mean ± SD from three independent replicates ($n=3$). Different superscript letters indicate significant differences at $p < 0.05$ according to one-way ANOVA followed by Tukey's post hoc test. All values are expressed on a fresh weight (FW) basis.

Effect of treatment on ash content. The interaction between B and Zn slightly influenced ash levels across treatments ($p < 0.05$). The control group exhibited 9.5 % ash, while Zn at 10 mg kg^{-1} slightly increased ash content to 9.6 %, possibly reflecting a hermetic response, where low Zn stimulates root activity and mineral deposition [21]. In contrast, all other treatments reduced ash content, as listed in **Table 5**. B at 15-20 mg kg-^{1} decreased values to 6.6 and 6.3 %, showing a 30 -34 % decline relative to control. Co-application of B + Zn at 15 mg kg^{-1} yielded 6.6%, while 20 mg kg^{-1} suppressed ash content further to 5.7 %, a -40 % reduction relative to control. At 25 mg kg^{-1} B + Zn, ash content partially recovered to 7.4%, but remained 22 % lower than control.

Table 5. Ash content of *B. rapa* L. roots cultivated under B, Zn, and combined B + Zn treatments at concentrations of 10, 15, 20, and 25 mg kg^{-1}.

Groups	Control	10 mg kg^{-1}	15 mg kg^{-1}	20 mg kg^{-1}	25 mg kg^{-1}
Boron	9.5 ± 0.1 ^{a}	5.5 ± 0.0 ^{c}	6.6 ± 0.0 ^{bc}	6.3 ± 0.0 ^{bc}	6.9 ± 0.2 ^{b}
Zinc		9.6 ± 0.0 ^{a}	6.7 ± 0.0 ^{bc}	6.0 ± 0.0 ^{bc}	6.9 ± 0.2 ^{b}

Boron + Zinc	6.9 ± 0.2 [b]	6.6 ± 0.0 [bc]	5.7 ± 0.0 [c]	7.4 ± 0.2 [b]

Values are presented as mean ± SD from three independent replicates ($n=3$). Different superscript letters indicate significant differences at $p < 0.05$ according to one-way ANOVA followed by Tukey's post hoc test. All values are expressed on a fresh weight (FW) basis.

Effect of treatment on dietary fiber content. Dietary fiber content was significantly influenced by micronutrient treatments ($p < 0.01$), showing a concentration-dependent response (**Table 6)**. The control group exhibited 11.3 %, while the highest value observed under B + Zn co-application at 10 kg mg^{-1} (12.8 %), a 13.3 % increase relative to the control. This treatment was statistically significant compared to both control and individual micronutrient applications. In contrast, B + Zn at 15 mg kg^{-1} (10.2 %) and 25 mg kg^{-1} (11.5 %) did not differ significantly from the control, showing that the synergistic effect is most pronounced at lower concentrations. Zn alone induced a moderate but non-significant increase (11.2 % at 15 mg kg^{-1}), while B alone showed variable results ranging from 9.7 to 13.2 %.

Table 6. Dietary content of *B. rapa* L. roots cultivated under B, Zn, and combined B + Zn treatments at concentrations of 10, 15, 20, and 25 mg kg^{-1}.

Groups	Control	10 mg kg^{-1}	15 mg kg^{-1}	20 mg kg^{-1}	25 mg kg^{-1}
Boron		10.1 ± 0.0 [b]	13.2 ± 0.0 [a]	9.7 ± 0.1 [b]	10.3 ± 0.0 [b]
Zinc	11.3 ± 0.0 [ab]	9.2 ± 0.0 [b]	11.2 ± 0.0 [ab]	9.9 ± 0.1 [b]	9.9 ± 0.0 [b]
Boron + Zinc		12.8 ± 0.0 [a]	10.2 ± 0.0 [b]	10.0 ± 0.0 [b]	11.5 ± 0.2 [ab]

Values are presented as mean ± SD from three independent replicates ($n=3$). Different superscript letters indicate significant differences at $p < 0.05$ according to one-way ANOVA followed by Tukey's post hoc test. All values are expressed on a fresh weight (FW) basis.

Effect of treatment on fat content. Fat and phenolic contents were quantified to elucidate the role of micronutrient supplementation on lipid metabolism and antioxidant potential in *B. rapa* L. **(Table 7).** Fat contents varied across treatments ($p > 0.05$). The control group exhibited 2.5 %, while Zn application at 15 mg kg^{-1} increased fat content to 2.7 % (+8% relative to control), showing the highest value among single-element treatments. In contrast, Zn at 10 and 20 mg kg^{-1} reduced fat to 1.0% and 0.8%, respectively, while 25 mg kg^{-1} maintained a low level (1.3%). B treatments showed a concentration-dependent decline, with values ranging from 2.2% at 10 mg kg^{-1} to 0.9% at 25 mg kg^{-1}, showing suppression of lipid accumulation at higher doses. Combined B + Zn application produced variable results: 1.5% at 10 mg kg^{-1}, 1.9 at 15 mg kg^{-1}, and a sharp decline to 0.2% at 20 mg kg^{-1}, before partial recovery at 25 mg kg^{-1} (1.2%).

Table 7. Fat content of *B. rapa* L. roots cultivated under B, Zn, and combined B + Zn treatments at concentrations of 10, 15, 20, and 25 mg kg^{-1}.

Groups	Control	10 mg kg^{-1}	15 mg kg^{-1}	20 mg kg^{-1}	25 mg kg^{-1}
Boron		2.2 ± 0.0 [a]	1.0 ± 0.0 [b]	1.4 ± 0.1 [b]	0.9 ± 0.0 [b]
Zinc	2.5 ± 0.0 [a]	1.0 ± 0.0 [b]	2.7 ± 0.0 [a]	0.8 ± 0.0 [b]	1.3 ± 0.0 [b]
Boron + Zinc		1.5 ± 0.0 [b]	1.9 ± 0.0 [b]	0.2 ± 0.0 [c]	1.2 ± 0.0 [b]

Values are presented as mean ± SD from three independent replicates ($n=3$). Different superscript letters indicate significant differences at $p < 0.05$ according to one-way ANOVA followed by Tukey's post hoc test. All values are expressed on a fresh weight (FW) basis.

Effect of treatment on phenolic contents. Phenolic content in *B. rapa* L. roots exhibited a concentration-dependent response to micronutrient supplementation, as shown in **Fig. 1**. The control group showed the highest phenolic level (1.9 mg GAE g^{-1} FW), while all treatments produced comparatively lower phenolic levels. B alone showed only modest changes, ranging between 0.3-0.4 mg GAE g^{-1} FW, showing that B does not strongly activate phenolic biosynthesis. In contrast, Zn treatment produced variable results, with the lowest value at 15 mg kg^{-1} (0.1 mg GAE g^{-1} FW) and the highest at 20 mg kg^{-1} (1.1 mg GAE g^{-1} FW), a 42% reduction compared to the control, but still higher than the B alone treatment.

The co-application of B and Zn revealed a concentration-dependent pattern. At 15 mg kg^{-1}, phenolic content reached 1.6 mg GAE g^{-1} FW, which, although lower than control, was significantly higher than B or Zn alone treatments ($p < 0.05$). At 20 mg kg^{-1}, phenolic level declined to 0.4 mg GAE g^{-1} FW, showing that beyond moderate concentration, micronutrient synergy is lost or antagonistic. This strong B × Zn interaction ($p < 0.01$) shows that phenolic induction is not additive, with optimal induction occurring at moderate co-application levels.

Fig. 1

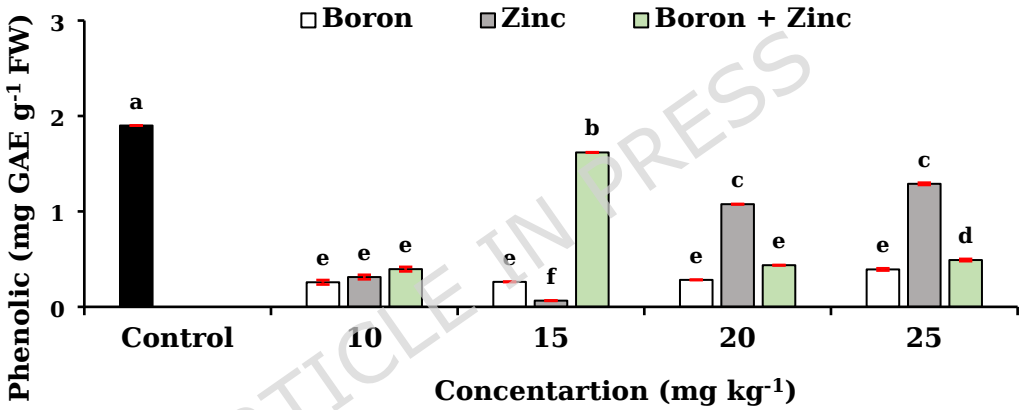

Figure 1. Total phenolic content (mg GAE g^{-1} FW) of *B. rapa* L. roots cultivated under B, Zn, and combined B + Zn supplementation (control, 10, 15, 20, 25, mg kg^{-1}). Total phenolics were quantified using gallic acid standard curve and expressed as milligrams of gallic acid equivalents (GAE) per gram fresh weight (FW). All data are expressed as mean ± SD values from three independent experiments *(n =3)*. Different lowercase letters above bars indicate statistically significant differences among treatments based on ANOVA followed by Tukey's HSD

Nutritional variability by phenolic and protein content in *B. rapa* L. under B and Zn supplementation. Principal component analysis (PCA) revealed a distinct clustering pattern among treatments, as shown in **Fig. 2**. The combined micronutrient supplementation (B + Zn) at 15 mg kg^{-1} showed a strong positive association with protein and ash contents, showing a synergistic enhancement of N metabolism and mineral deposition. Moisture and fats clustered closely with the B15 (15 mg kg^{-1}) and B + Zn25 (25 mg kg^{-1}), which demonstrates regulation of water retention and lipid metabolism under moderate supplementation. In contrast, phenolic compounds exhibited a strong association with the control and B + Zn 15 (mg kg^{-1}) treatments, consistent with their role in secondary metabolites production under limited Zn levels. Protein content clustered in Zn (20-25 mg

kg^{-1}) treatments, where amino acid metabolism and protein biosynthesis were stimulated at higher Zn concentrations. PCA further confirmed a significant B × Zn interaction effect ($p < 0.05$) affecting fiber, ash, and phenolic traits. PC1 and PC2 explained 26.57 % and 24.49 % of the total variance, respectively. Overall, the nutritional hierarchy based on PCA analysis is: Control > phenolic accumulation, while B + Zn (moderate levels) > protein and ash enrichment (synergistic metabolic regulation).

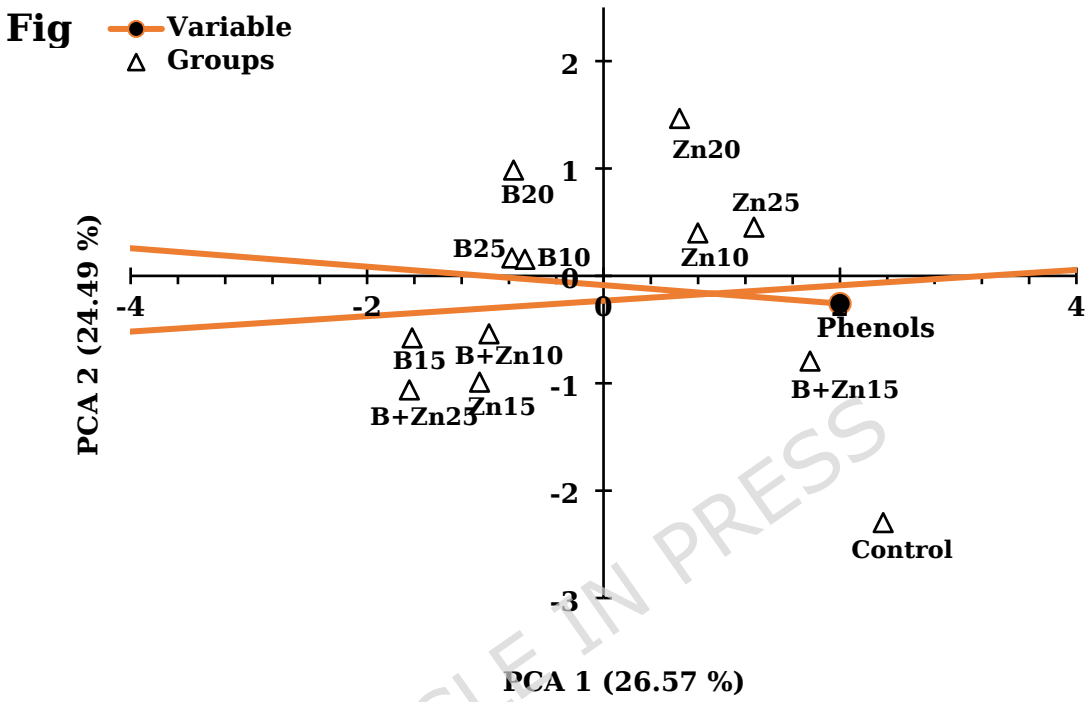

Figure 2. Principal Component Analysis (PCA) biplots showing the effects of individual and combined B, Zn, and B + Zn treatments on the nutritional composition of *B. rapa* L. The plot shows the relationship between treatments and key nutritional components. Nutritional components (fiber, protein, fats, moisture, phenols, and ash) are represented as vectors. The control treatment was plotted separately. The variation is explained by the two PCA components (Components 1 and 2). Data represent mean values from three independent biological replicates ($n = 3$).

Aflatoxin B1 (AFB_1) detoxification under B and Zn. AFB_1 detoxification in *B. rapa* L. roots showed a concentration-dependent response to micronutrient supplementation, as shown in **Fig. 3A-D**. The control group maintained the highest AFB_1 (24 µg kg^{-1}), while individual B and Zn treatments at 10-15 mg kg^{-1} reduced AFB_1 to 10-12 µg kg^{-1}, equivalent to a 58.85 % reduction, relative to the control. The combined B + Zn treatment at 15 mg kg^{-1} produced the most pronounced effect, lowering AFB_1 to 10 µg kg^{-1}, equivalent to a 60.08 % reduction compared to the control. At higher concentration, detoxification efficiency declined: B + Zn at 20 mg kg^{-1} unexpectedly increased AFB_1 to 29 µg kg^{-1}, while at 25 mg kg^{-1}, B + Zn reduced AFB_1 to 14 µg kg^{-1}, still lower than the control but less effective compared with the 15 mg kg^{-1} treatment groups.

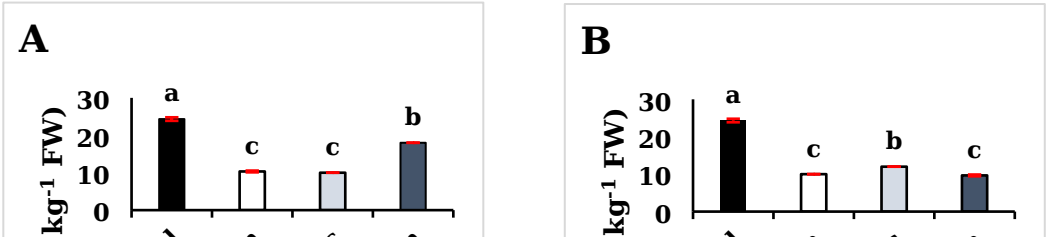

B-Zn synergy enhances stress tolerance and productivity in *B. rapa* L. The combined application of B and Zn at 15-20 mg kg^{-1} consistently achieved the highest stress tolerance index (STI) and geometric mean productivity (GMP) across all biochemical traits. B + Zn at 20 mg kg^{-1} showed higher values in dry matter and phenolic, alongside high GMP values, as shown in **Fig. 4A**. In contrast, Zn alone treatment at 25 mg kg^{-1} produced superior STI and GMP in protein and fiber. B treatments (10-25 mg kg^{-1}) induced only modest increases in STI; nonetheless, associated with relatively low GMP, as shown in **Fig. 4B**. Across traits, STI and GMP were strongly correlated. Consistent patterns were observed in the relative performance index (RPI), where B + Zn at 15-20 mg kg^{-1} produced consistently positive values for dry matter, protein, phenolics, and AFB_1 mitigation (**Fig. 4C)**. These RPI values closely align with STI and GMP score, showing the synergistic effect of co-application. However, tolerance index (TOL) values were strongly negative under all individual Zn and combined B + Zn treatments, except at 20 mg kg^{-1} of B + Zn. Micronutrients co-application also enhanced the yield stability index (YSI) and is considered a critical measure of performance for NFE, protein, dry matter, and ash content, as shown in **Fig. 4E**.

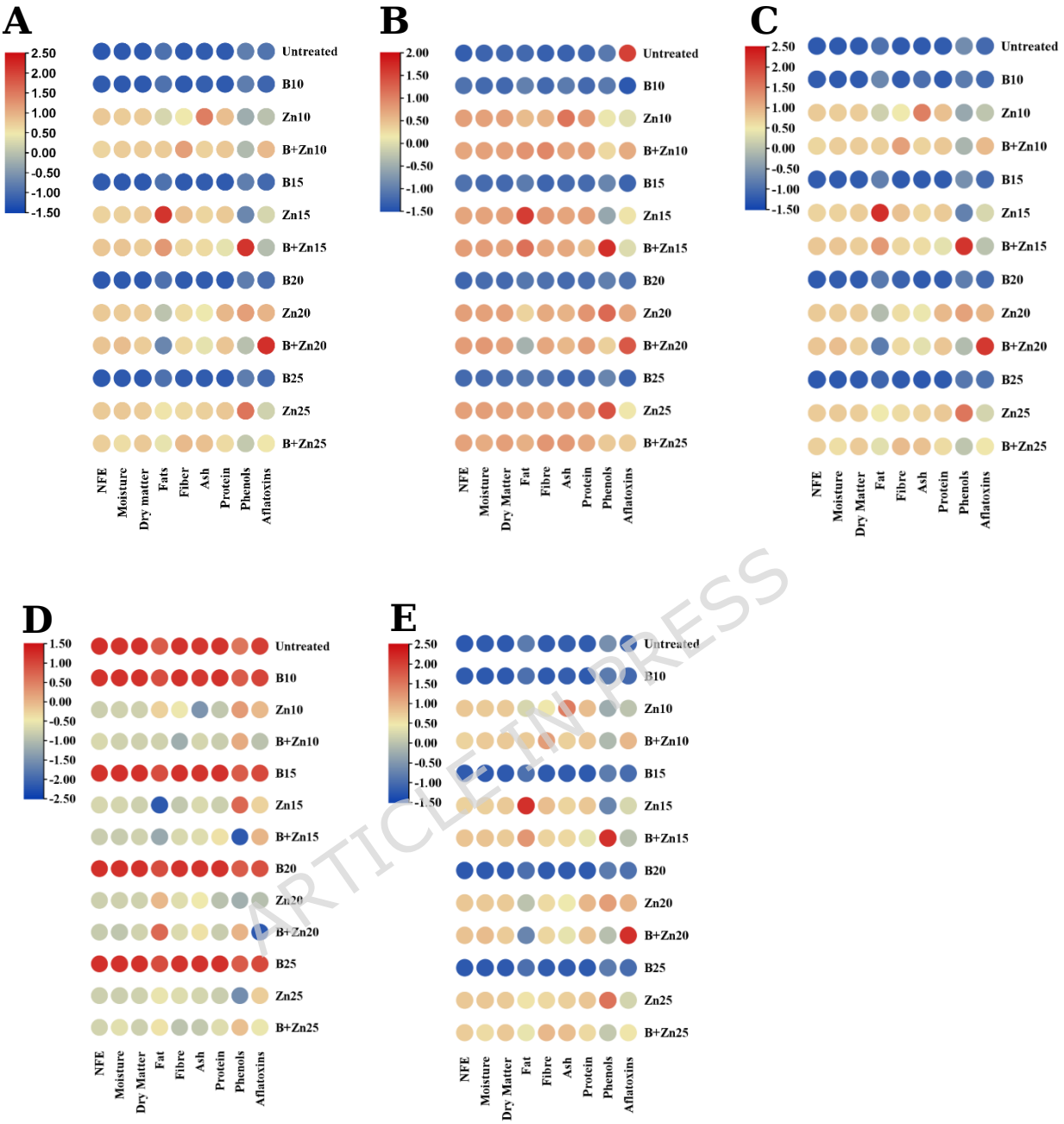

Figure 4. Heatmap of stress related indices in *B. rapa* L. root under micronutrient supplementation.
(A) Tolerance Index (STI), **(B)** Geometric Mean Productivity (GMP), **(C)** Relative Performance Index (RPI), **(D)** Tolerance Index (TOL) **(E)** Yield Stability Index (YSI) across treatments with Boron (B10 to B25), Zinc (Zn10 to Zn25), and their combination B + Zn (B + Zn10 to B + Zn25), relative to control. Indices were calculated for nine key biochemical traits (NFE, moisture, dry matter, fat, fiber, ash, protein, phenols, and AFB_1). **Color gradients:** orange to deep red = high values

Discussion. Edible roots of *B. rapa* L. root (turnip) represent a direct dietary source, making both nutritional enhancement and toxin suppression critical for food safety. The present study shows that balanced co-application of B and Zn not only improved nutritional traits and biomass but also reduced AFB_1 contamination. In public health, MTs are a major health

concern in edible crops alongside unsafe food and water [22] [23]. Thus, during this study, in a concentration-dependent manner, the treatments of B and Zn (10-25 mg kg^{-1}) were applied. The combination of Zn and B at 15-20 mg kg^{-1} was associated with enhanced nutritional traits and AFB_1 suppression. This dual result arises from micronutrient synergy: B stabilizes cell walls and fiber deposition, limiting fungal penetration, while Zn activates antioxidant enzymes that detoxify ROS and biosynthesize AFB_1. The co-application of B and Zn enhances photosynthetic efficiency and antioxidant defense, thereby increasing carbohydrate availability [24]. The NEF fraction, composed primarily of soluble sugars, reflected this effect: synergy at 20 mg kg^{-1} maximizes enzymatic activity, consistent with Zn's catalyst role in carbonic anhydrase [25], and B function in phloem integrity and sugar-borate formation [16]. In root crops, the B-Zn interaction upregulated the sucrose transporter gene (*SUTs*) [26], correlating with the observed increase in NFE at the 20 mg kg^{-1} group. At higher concentration (25 mg kg^{-1}), NFE declined, showing a shift from synergy to antagonism due to disrupted lignification and metabolic homeostasis [27]. Thus, these findings define 15-20 mg kg^{-1} as the optimal metabolic window for NFE accumulation in *B. rapa* L.

B and Zn supplementation support osmotic regulation, cellular turgidity, and structural carbohydrate biosynthesis, processes that underpin dry matter accumulation. Previous studies report that B treatment enhances root dry matter in *Brassica napus* (canola), while Zn promotes carbohydrate partitioning in *Raphanus sativus* (radish) [28]. Similarly, foliar B + Zn application has been shown to increase biomass and root yield in *B. rapa* under variable irrigation frequencies [29]. In our study, only at 25 mg kg^{-1} co-application, exceeding both control and single treatments. This improvement likely contributes to greater root stability and nutrient utilization efficiency, with potentially implications for extending post-harvest shelf life. Such outcomes align with integrated micronutrient management strategies that optimize yield and storage quality in nutrient-deficient soils, as shown in *Solanum tuberosum* L. (potato) species [30]. Further, moisture content in *B. rapa* L exceeded values reported in *Ensete ventricosum* (Ethiopian banana) [31], with discrepancies attributed to soil nutrient deficiency and agronomic practices. Co-application of B and Zn enhanced water-retention, supporting the activity of soluble enzymes and coenzymes essential for metabolism [32]. Elevated moisture also facilitates hydrogen cyanide (HCN) detoxification via glycosidase activity [33]. However, while moderate supplementation (20 mg kg^{-1}) maximized moisture content, excessive supplementation application (25 mg kg^{-1}) reduced retention, showing that localized stress affects the benefits of micronutrient synergy. In this study, protein content exhibited a biphasic response to micronutrient supplementation, and low-level co-application impaired N assimilation, whereas moderate to high concentrations enhanced protein content. Individual B supplementation promoted amino acid synthesis and stress tolerance [34], while Zn activated key enzymes in protein biosynthesis [25]. Previous studies confirm that Zn deficiency disrupts N metabolism in maize [35], while supplementation enhances protein synthesis in *Vigna radiata* L. (mung bean) [36]. Cross-talk between macro-micro nutrient uptake pathways has been reported [28] [37], showing the balance required between N metabolism and micronutrient availability. Our results extend this evidence to *B. rapa* L., proving that synergistic B + Zn application at elevated levels supports N metabolism and protein accumulation. In mineral deposition (ash content), the inhibitory effect was observed at moderate to high co-application levels. B influences mineral transport and absorption within the cell wall [38], while Zn variably affects mineral uptake depending on concentration [39] [40]. Our results contrast with earlier reports of enhanced mineral redistribution under B supplementation [41], instead aligning with evidence that high B + Zn levels can cause ionic competition at uptake sites. Thereby limiting mineral accumulation [42]. Similar inhibitory interactions have been observed in our prior study [17]. These findings suggest that while elevated B + Zn enhances protein metabolism, it simultaneously suppresses mineral deposition. Further prioritizing the tradeoff between N assimilation and mineral balance in the *B. rapa* L. root.

Micronutrient co-application influenced both structural carbohydrate deposition and lipid metabolism. Fiber enrichment under combined treatment likely reflected B-facilitated pectin cross-linking via borate diester bonds and Zn-mediated activation of glycosyltransferases (GTs), which together support polysaccharide assembly in the primary cell wall [16]. Zn also contributes to carbohydrate metabolism and energy transfer, indirectly supporting cell wall thickening [43]. The significant B × Zn interaction ($p < 0.01$) confirms a synergistic effect, with moderate co-application enhancing fiber content, while higher concentrations suppressed or plateaued the response. Similarly, fat content exhibited a concentration-dependent biphasic pattern. Zn stimulated acetyl-CoA carboxylase (ACA) activity, a key enzyme in fatty acid synthesis [16]. In contrast, B supplementation alone produced variable results. Moderate co-application supported lipid accumulation. Nonetheless, excessive supplementation disrupted lipid homeostasis, consistent with prior reports of Zn-mediated regulation of lipid metabolic pathways [16]. These findings highlight the threshold-dependent nature of B and synergy, in which a moderate level enhances both fiber biosynthesis and fatty acid metabolism.

Phenolic enrichment under Zn and B + Zn supplementation reflects activation of the phenylpropanoid pathway, which governs polyphenolic biosynthesis. In *B. rapa* L. sprouts, phenolic accumulation is closely coupled to glucosinolate metabolism, showing their dual role in defense and dietary bioactivity [44]. Comparative analyses across *Brassica* vegetables further emphasize phenols as undervalued phytonutrients with profound implications for human health, especially in mitigating oxidative stress [45]. Metabolomic profiling further shows that micronutrient modulation selectively enhances phenolic biosynthesis and confers adaptive advantages under stress conditions [46]. In our study, while the control group maintained the highest phenolic levels, Zn and B + Zn supplementation at optimal concentration improved phenolic accumulation relative to single-nutrient treatments. Notably, combined B + Zn at 15 mg kg^{-1} was more effective than individual Zn at higher concentrations in enhancing N assimilation. This diversion of phenylalanine toward protein synthesis rather than the phenylpropanoid pathway reduced phenolic content despite increased protein levels [47]. Such metabolic trade-offs reinforce the antioxidant potential of B + Zn synergy and contribute to stress resilience and AFB_1 detoxification in *B. rapa* L. Micronutrient regulation is central to plant growth and nutritional composition [48]. While the individual roles of B and Zn are well known, their combined impacts in *B. rapa* L. remain inadequately explored. This study addressed that gap by evaluating both single and co-application across multiple parameters. The results showed that multi-elemental synergy catalyzes nutritional enrichment through coordinated regulation of metabolic flux pathways [49].

A striking result was observed in AFB_1 detoxification, at 20 mg kg^{-1}, B + Zn, paradoxically increased AFB_1 levels above the control. This threshold beyond which synergy is lost, potentially due to metabolic imbalance or iron (Fe) antagonism [50]. In contrast, moderate co-application (10-15 mg kg^{-1}) markedly reduced AFB_1 accumulation with the 15 mg kg^{-1} treatment, achieving the strongest detoxification effect. These findings show the concentration-dependent manner of micronutrient interactions, where balanced supplementation sustains bio-enzymatic detoxification pathways; nevertheless, excess disrupts redox homeostasis. Zn contributes via *SOD* activity [51], while B enhances resilience against fungal pathogens and abiotic stressors [52], thereby reducing aflatoxin biosynthesis. The translational relevance of these results is reinforced by animal and human studies. Dietary Zn supplementation in livestock mitigates AFB_1-induced oxidative stress, improves hepatic function, and lowers DNA adduct formation [53]. Similarly, B supplementation in rodent models alleviates mycotoxin-induced immunosuppression and genotoxicity [54]. Human studies further reveal a negative correlation between aflatoxin exposure and serum Zn levels in children, identifying Zn deficiency as a risk factor for heightened AFB_1 toxicity [42].

These synergistic effects of B and Zn are consistent with a prior study in canola, in which combined fertilization significantly improved growth and yield metrics [55]. In *Brassica* species, Zn co-application has been shown to enhance drought and salinity

resilience by preserving chlorophyll integrity and boosting antioxidant defense systems, *i.e., CAT, POD,* and *APX* activities [56]. In contrast, B alone exerted minimal influence on antioxidant defense in *Beta vulgaris* (sugar beet) inoculated with *Athelia rolfsii* (white mold), whereas Zn or combined B + Zn treatments were more effective [57]. Our findings align with these reports, showing that integrated B and Zn supplementation optimizes nutrient metabolism, mitigates stress effects, and enhances detoxification mechanisms. Consistent patterns were observed in *B. napus* L., where B + Zn co-application enhanced antioxidant enzyme activity and improved physiological stability [55]. Zn alone fortified membrane integrity and upregulated stress-response osmolyte production [58]. To capture resilience beyond single-trait measurement. We applied integrated stress indices to evaluate productivity, sensitivity, and stability under micronutrient supplementation. Previous findings have shown the relevance of such stability metrics in breeding for environment-resilient crops [59], and co-application of B and Zn has been shown to enhance physiological stability and stress recovery in mustard and oilseed crops [60]. In our study, treatment with 15 mg kg^{-1} Zn and 20 mg kg^{-1} B + Zn provided the most favorable combination of high productivity (STI, GMP), low stress sensitivity (RPI, TOL), and high yield stability (YSI). These results confirmed a synergistic interaction between B and Zn in sustaining yield and physiological consistency under metal-induced stress. Elevated YSI values were observed under Zn alone and combined B + Zn at 10 -20 mg kg^{-1}. Particularly across NFE, protein, dry matter, and ash content. These values reflect the treatments' capacity to maintain trait expression and minimize yield deviation compared to non-stressed conditions. YSI was particularly robust when interpreted alongside productivity indices (STI, GMP), together showing stability and performance. Notably, *B. rapa* L., with high YSI, also showed stronger suppression of AFB_1 accumulation. This further suggests that biochemical stability and enhanced detoxification potential are linked to micronutrient-induced antioxidant activation. In comparison, detoxification mechanisms have been reported in microbial systems, showing potential resilience through enhanced metal tolerance [61] and pathogen tolerance [62].

Conclusion. This study established a definitive concentration-dependent hierarchy for the synergistic application of B and Zn in enhancing the nutritional composition and biochemical stability of *B. rapa* L. roots. Our result identifies the 15-20 mg kg^{-1} B + Zn range as the optimal range for metabolic processes, establishing a hierarchy of B + Zn > B > Zn. Crucially, co-application at 15 mg kg^{-1} mitigates food safety risks by achieving the maximum AFB_1 suppression, while simultaneously priming phenolic biosynthesis. At 20 mg kg^{-1}, the treatment optimized carbohydrate and lipid metabolism, significantly increasing both NFE and fat accumulation ($p < 0.05$). The peak STI and RPI values under moderate supplementation show a state of physiological resilience, likely driven by improved metabolic balance and potent antioxidant activation. Conversely, lower doses primarily improved structural development, while excessive supplementation triggers a physiological threshold effect. The convergence of protein, lipid, and phenolic profiles under co-application validates this approach as a superior alternative to individual micronutrient applications. These findings position balanced B-Zn application (15 -20 mg kg^{-1}) as a robust strategy for enhancing nutrient metabolism and AFB_1 resistance. Future research is essential to elucidate the regulatory gene networks and molecular signaling pathways of B-Zn synergy for long-term crop resilience.

Limitations of the study. The study elucidated the effect of B and Zn supplementation on nutritional quality and AFB_1 contamination in *B. rapa* L. roots, but did not investigate the underlying molecular pathway. Specifically, gene expression related to detoxification was not assessed. Future research will incorporate RT-qPCR to quantify detoxification-related gene expression and evaluate its regulation under B-Zn co-treatment. Additionally, transcriptomic and proteomic approaches will be employed to uncover broader regulatory networks influenced by B-Zn synergy, providing mechanistic insight into stress adaptation and toxin suppression.

Materials and Methods

Preparation of the soil for the cultivation of *B. rapa* L. seeds. Air-dried silt loam soil was collected from the experimental research farm of Abdul Wali Khan University, Mardan (AWKUM), Pakistan, with a long-term history of cultivation. Soil samples were collected from the top 0-25 cm depth (active root zone). Further, the soil was sieved through a 5-mm mesh and divided into separate 1-kg portions for each group: zinc (Zn), boron (B), and a combined Zn + B application. Zn was supplied as zinc sulfate heptahydrate ($ZnSO_4 \square 7H_2O$), and B as boric acid (H_3BO_3). Treatments were applied at four concentration levels: 10, 15, 20, and 25 mg kg^{-1} of soil. In the Zn + B group, each dose consisted of equal concentrations of Zn and B (e.g., 10 mg kg^{-1} Zn + 10 mg kg^{-1} B). Untreated soil was analyzed for baseline concentrations of several metals, including Ni, Zn, Cd, Cr, Fe, Pb, Ca, Mg, and Mn, using atomic absorption spectrometry (AAS) **(Supplementary Table S1).** Although the soil was not sourced from a certified contaminated site, residual metal content was present due to prior field use. After the amendment, soils were thoroughly homogenized and re-sieved before potting. Each treatment, including the non-amended control, was replicated more than three times (minimum triplicate, with additional replicates for statistical reliability). The experiments were conducted over one growing season (single-year data). Plants were cultivated in plastic pots (15-cm diameter × 20-cm height), each filled with 1 kg of treated soil. All pots were maintained under controlled greenhouse conditions, ensuring uniform irrigation and temperature throughout the experiment [17]. The rationale for selecting only Zn and B was based on their critical role in plant nutrition, stress physiology, and detoxification pathways, particularly in *B. rapa* L. However, other micronutrients were not supplemented during this work.

Preparation of *B. rapa* L. seeds for cultivation. Seeds of *B. rapa* L. (var. Maqsood) were purchased from the Institute of Biotechnology and Genetic Engineering (IBGE), University of Agriculture, Peshawar, Pakistan. The cultivation experiments were conducted at the Department of Botany, Abdul Wali Khan University, Mardan (34.2131° N, 72.0680° E). The seeds were surface-sterilized in 30% hydrogen peroxide (H_2O_2) for 15 minutes, as this concentration is widely reported to effectively eliminate surface pathogens while maintaining seed viability. However, higher concentrations (>30%) can cause oxidative damage to the seed coat and embryo, resulting in reduced germination, abnormal seedling development, or loss of viability [63]. Further, the samples were carefully washed with deionized water. These disinfected seeds of *B. rapa* L. were then germinated on moistened filter paper placed in Petri dishes. The germination chamber was maintained at 25 ± 1°C with a 16/8 h light/dark photoperiod and a light intensity of approximately 150 µmol m^{-2} s^{-1}. Relative humidity was maintained at approximately 70%, and filter papers were re-moistened daily to ensure consistent hydration. After four days, uniformly germinated healthy seedlings measuring approximately 3-5 cm in height and bearing one to two leaves were selected for transplantation into prepared pots. Plants were cultivated in a climate-controlled greenhouse, where temperature (25 °C Day / 19 °C night), relative humidity (52%), and a 12-h photoperiod were actively maintained throughout the experiment. Seedlings were irrigated with distilled water throughout the experiment. Each pot received 100 mL of distilled water every two days, adjusted as needed to maintain consistent soil moisture without waterlogging. Each pot was regularly rotated to ensure uniform exposure to light and temperature. Irrigation volumes were determined based on preliminary trials and monitored visually to ensure uniform hydration across treatments. Two weeks after cultivation, the aboveground parts of *B. rapa* L. plants were harvested and washed with distilled water to remove any adhering soil particles [17].

Preparation and collection of *B. rapa* L. root sample. To evaluate the biochemical composition of *B. rapa* L. roots cultivated under varying concentrations of Zn and/or B (10, 15, 20, and 25 mg kg^{-1}), harvested roots were thoroughly washed to remove residual soil, and the outer epidermal layer was carefully peeled. The remaining edible tissue was homogenized using a high-speed blender. Further, roots were pooled to obtain 100 g of homogenized pulp, based on individual root size and mass. To ensure uniformity in analytical measurement, the pulp was finely ground and sieved to achieve a consistent particle size distribution of 500 µm. To preserve biochemical and structural integrity, samples were vacuum-sealed in sterile polyethylene bags and stored at -18 °C. All samples were processed for biochemical analysis within two weeks of harvest to ensure stability and reproducibility [17].

Determination of aflatoxin B_1 (AFB_1) content. To quantify AFB_1 levels in *B. rapa* L. roots cultivated under B and Zn, and combined B + Zn supplementation, a modified enzyme-linked immunosorbent assay (ELISA) protocol was employed [64]. Briefly, harvested root samples were washed and homogenized in a methanol: water solution (70:30, v/v). The homogenate was filtered through Whatman No. 1 filter paper and centrifuged at 10,000 rpm for 10 min at 4 °C. The resulting clear supernatant

was collected for AFB_1 analysis. Quantification was performed using a commercial ELISA kit specific for AFB_1 detection (Euro Proxima, Austria), following the manufacturer's instructions. The kit's detection limit was <1.0 µg kg^{-1}, with a recovery range of 85-100% validated for food matrices [65]. Absorbance was measured at 450 nm using a microplate spectrophotometer (Thermo Scientific, USA). A standard calibration curve was constructed using AFB_1 standard ranging from 0 to 10 ppb. Linear regression (R^2 = 0.99) was applied to derive the quantification equation, and sample concentrations were calculated accordingly and expressed in µg g^{-1} fresh weight (FW).

Moisture determination in *B. rapa* L. Moisture content of *B. rapa* L., root samples cultivated under varying concentrations of B and/or Zn (10, 15, 20, and 25 mg kg^{-1}) was determined using standardized methods of the Association of Official Analytical Chemists (AOAC 925.10) [66]. Briefly, moisture content was measured by oven-drying of 2 g of fresh root tissue weighed on an analytical balance (± 0.001g) in a hot air oven (Mummert UN110, Germany) at 105 °C until a constant weight was achieved. Constant weight was confirmed by repeated weighing at 30-minute intervals, and samples were cooled in a desiccator before final weighing to prevent moisture reabsorption. Moisture percentage was calculated as (FW-DW/FW) × 100, and results were expressed as a percentage of fresh weight (FW, wet basis). All samples were prepared immediately after harvest, vacuum-sealed, and stored at -18 °C until analysis to ensure reproducibility.

Crude protein quantification in *B. rapa* L. Crude protein of *B. rapa* L., root under varying concentrations of B and/or Zn at 10, 15, 20, and 25 mg kg^{-1} was determined by the AOAC (984.13) Kjeldahl method [66]. Briefly, crude protein content was quantified using 0.5 g powdered samples digested with concentrated H_2SO_4 and catalyst tablets (K_2SO_4 + $CuSO_4$). After complete digestion, the samples turned a clear light green, indicating successful breakdown of organic matter. Further, distillation was performed using a Behr Kjeldahl unit, with ammonia trapped in boric acid solution. All titrations were carried out using standardized 0.1 N HCL. The total nitrogen (%) was calculated as [(sample titre – blank titre) × normality × 1.4] / sample weight, with all weights recorded on an analytical balance (± 0.001 g). Crude protein (%) was obtained by multiplying total nitrogen by 6.25, and values were expressed on fresh weight (FW, wet basis). All samples were vacuum-sealed and stored at -18 °C until analysis to prevent degradation.

Estimation of total fat content in *B. rapa* L. Total fats of *B. rapa* L., root samples under varying concentrations of B and Zn (10, 15, 20, and 25 mg kg^{-1}) were determined using the hydrolysis method (AOAC 984.15) [66]. Briefly, 2 g of the sample was treated with 4 N HCL and refluxed for 1 h. Lipids were extracted using a Soxhlet extractor (Gerhardt, Germany) with petroleum ether (boiling range 40 - 60 °C). The extract was evaporated at 60 °C, and the residue was weighed to a constant mass and the residue was weighed to a constant mass after cooling in a desiccator to prevent moisture absorption. Fat (%) was calculated as [(extract weight/sample weight × 100)], and values were expressed on a fresh weight (FW, wet basis). Vacuum-sealed samples were stored at -18 °C until analysis to ensure reproducibility.

Dietary fiber assessment in *B. rapa* L. Dietary fibers of *B. rapa* L., root under varying concentrations of B and Zn (10, 15, 20, and 25 mg kg^{-1}) were determined using the enzymatic gravimetric method (AOAC 991.43) [67]. Briefly, sequential digestion was performed with alpha-amylase (pH 6.0, 95 °C) for 30 min, protease (pH 7.5, 60 °C) for 30 min, and amyloglucosidase at 60 °C, pH 4.5 for 30 min. Fiber was precipitated with 95 % ethanol, then filtered, dried at 105 °C, and weighed. The residue was cooled in a desiccator before final weighing to prevent moisture reabsorption. Fiber (%) was calculated as [(residue weight – protein – ash) / sample weight × 100], and values were expressed on a fresh weight (FW wet basis). Samples were sealed under vacuum and preserved at -18 °C until analysis to ensure reproducibility.

Ash content measurement in *B. rapa* L. To further understand the mineral composition and nutritional stability of *B. rapa* L. root. Ash content was determined under varying concentrations of B and Zn (10, 15, 20, and 25 mg kg^{-1}) using the gravimetric method (AOAC 923.03) [66]. Briefly, 2 g of powdered root samples was incinerated in a muffle furnace (Nab retherm L9/11/B170, Germany) at 550 °C for 6 h. The stable residues were cooled in a desiccator to prevent moisture absorption. Ash (%) was calculated as [(residue weight/sample weight) × 100], and values were expressed on a fresh weight (FW, wet basis). All samples were prepared immediately after harvest, vacuum-sealed, and stored at -18 °C until analysis to ensure reproducibility.

Determination of total carbohydrate in *B. rapa* L. Total carbohydrate content of *B. rapa* L. roots cultivated under varying concentrations of B and/or Zn (10, 15, 20, and 25 mg kg^{-1}) was determined by difference according to AOAC guidelines [66]. Carbohydrate (%) was calculated as: Carbohydrate (%) = 100 – (moisture + protein + fat + fiber + ash). All proximate values were expressed on fresh weight (FW, wet basis), and further samples were vacuum-sealed and stored at -18 °C until analysis to ensure reproducibility.

Caloric value estimation in *B. rapa* L. The caloric value (kcal/100 g) of *B. rapa* L. roots cultivated under varying concentrations of B and/or Zn (10, 15, 20, and 25 mg kg^{-1}) was estimated using Atwater conversion factors [66] [68]. Energy was calculated by assigning 4 kcal/g for protein and carbohydrates, and 9 kcal/g for lipids. The caloric values were obtained using the following equation: Energy (kcal/100 g) = (protein × 4) + (carbohydrate × 4) + (fats × 9). All proximate values were expressed on fresh weight (FW, wet basis). Samples were vacuum-sealed and stored at -18 °C until analysis to ensure reproducibility.

Determination of total phenolic content (TPC). Phenolic content of *B. rapa* L. root samples was determined using the Folin-Ciocalteu method [69]. Briefly, 0.5 g of powdered root tissue was extracted with 80% methanol and centrifuged at 10,000 rpm for 10 minutes. A 200 µL aliquot of the resulting supernatant was mixed with 1 mL of 10% Folin-Ciocalteu reagent and incubated for 5 minutes at room temperature. Subsequently, 800 µL of 7.5% sodium carbonate (Na_2CO_3) solution was added. The mixture developed a blue color, indicating phenolic compound presence. Further, the mixture was allowed to react or stabilize in the dark room for 30 minutes, and absorbance was measured at 765 nm using a UV-vis spectrophotometer (Thermo Scientific, USA). Result was expressed as mg gallic acid equivalents (GAE)/g fresh weight (FW, wet basis), calculated from a standard calibration curve ($R^2 > 0.99$).

Statistical analysis. All experimental data were initially recorded in Microsoft 365 (2024), and subsequently analyzed using IBM SPSS Statistics v.21. Results were expressed as mean ± standard deviations (SD), and triplicate assays were selected based on a validated AOAC protocol. Statistical power was confirmed via effect size and 95% confidence intervals. The use of three replicates *(n =3)* was chosen in line with AOAC standards as the validated minimum for proximate analysis, balancing reproducibility with feasibility. Further, data were assessed for normality and homogeneity of variance. ANOVA was performed on varying concentrations (10- 25 mg kg^{-1}) of B and Zn. Statistical significance differences among treatment means were determined using Tukey's post hoc test at $p < 0.05$. Pearson's correlation analysis was conducted to examine relationships among biochemical and nutritional traits, with significance set at $p < 0.05$, alongside PCA, multivariate patterns, and treatment clustering was performed using PAST software v.4.03.

Multivariate index analysis of *B. rapa* L. root. To further evaluate the physiological performance and yield stability of *B. rapa* L. under micronutrient treatments and stress conditions, five established agronomic indices were calculated using trait values under non-stressed (Yp) and stressed (Ys) conditions across treatments with B, Zn, and B + Zn at concentrations of 10, 15, 20, 25 mg kg^{-1}, following [70]. The indices included:

1. **Tolerance Index** (TOL = Yp – Ys), quantifying sensitivity to stress.
2. **Stress Tolerance Index** (STI = [Yp × Ys] / $[Yp]^2$], reflecting both yield potential and stress tolerance.
3. **Geometric Mean Productivity** (GMP = √ [Yp × Ys]), highlighting balanced performance under both conditions.
4. **Yield Stability Index** (YSI = Ys / Yp), indicating consistency under stress.
5. **Relative Performance Index** (RPI = Ys [treatment] / Ys [control]), comparing stressed yield performance relative to the untreated control.

Data availability

All data generated or analyzed during this study are included in this published article and its supplementary file.

Acknowledgements

None

Author contribution

Unays Siraj (U.S): Conceptualization, Data curation, Funding acquisition, Formal analysis, Investigation, Methodology, Project administration, Resources, Software, Supervision, Validation, Visualization, Writing – original draft.

Zainab Siraj (Z.S): Conceptualization, Data curation, Formal analysis, Investigation, Methodology, Writing – review & editing.

Patricio R. De Lo Rios-Escalante (P.D.L.R.E): Writing – review & editing, Funding acquisition.

Funding Declaration
This study was financially supported by Project MECESUP UCT 0804.

Declarations
Competing Interests
The authors declare no competing interests.
Ethics approval
No human or animal subjects were involved in this study
Additional Information
Supplementary Information: The online version contains supplementary materials available at
Correspondence and requests for materials should be addressed to U.S / unayskhan@gmial.com

References

1. Zhu, Z., Guo, W., Cheng, H., Zhao, H., Wanhj., Abdallah, M. F., Zhou, X., Lei., Tu, W., Wang, H., % Yang, J. Co-contamination and interactions of multiple mycotoxins and heavy metals in rice, maize, soybeans, and wheat flour marketed in Shanghai City. *J. Hazard. Mater.* **474**, 134695. https://doi.org/10.1016/j.jhazmat.2024.134695 (2024).
2. Taghizadeh, S. F., Tabriznia Tabrizi, G., Ahmadpourmir, H., Karimi, G. & Rezaee, R. Dietary exposure to aflatoxin B1, aflatoxin G1, ochratoxin A, and patulin through fruit juice consumption: A probabilistic assessment of health risk. *Toxicol. Rep.* **14**, 101894. https://doi.org/10.1016/j.toxrep.2025.101894 (2025).
3. Gemede, H. F. Toxicity, Mitigation, and Chemical Analysis of Aflatoxins and Other Toxic Metabolites Produced by Aspergillus: A Comprehensive Review. *Toxins 2025, Vol. 17, Page 331* **17**, 331. https://doi.org/10.3390/toxins17070331 (2025).
4. Jalili, C. Ranjbar Shamsi, R., Amiri, B., Kakebarbaie, S., Jalili, F., & Nasta, T. Z. Genotoxic and cytotoxic effects of aflatoxin on the reproductive system: Focus on cell cycle dynamics and apoptosis in testicular tissue. *Toxicology* **504**, 153773. https://doi.org/10.1016/j.tox.2024.153773 (2024).
5. Jin, J., Kouznetsova, V. L., Kesari, S., & Tsigelny, I. F. Synergism in actions of HBV with aflatoxin in cancer development. *Toxicology* **499**, 153652. https://doi.org/10.1016/j.tox.2023.153652 (2023).
6. Yang, X., Zhang, Q., Chen, Z. Y., Liu, H., & Li, P. Investigation of Pseudomonas fluorescens strain 3JW1 on preventing and reducing aflatoxin contaminations in peanuts. *PLoS One* **12**. https://doi.org/10.1371/journal.pone.0178810 (2017).
7. FAO/WHO Codex Alimentarius Commission. Codex Revision of Code of Practice for Aflatoxin B1 (CXC 45-1997). *Food and Agriculture Organization of the United Nations (FAO)* (2025).
8. Jobe, M. C., Mthiyane, D. M., Dludla, P. V., Mazibuko-Mbeje, S. E., Onwudiwe, D. C., & Mwanza, M. Pathological Role of Oxidative Stress in Aflatoxin-Induced Toxicity in Different Experimental Models and Protective Effect of Phytochemicals: A Review. *Molecules* **28**, 5369. https://doi.org/10.3390/molecules28145369 (2023).
9. Reverberi, M., Zjalic, S., Ricelli, A., Fabbri, A. A. & Fanelli, C. Oxidant/antioxidant balance inAspergillus parasiticus affects aflatoxin biosynthesis. *Mycotoxin Res.* **22**, 39–47. https://doi.org/10.1007/BF02954556 (2006).
10. Dineshkumar, R., Kumaravel, R., Gopalsamy, J., Sikder, M. N. A. & Sampathkumar, P. Microalgae as bio-fertilizers for rice growth and seed yield productivity. *Waste Biomass Valorization* **9**, 793–800. https://doi.org/10.1007/s12649-017-9873-5 (2018).
11. Zhang, Y., Jiang, Y., Gao, K., Sui, D., Yu, P., Su, M., Wei, G. W., & Hu, J. Structural insights into the elevator-type transport mechanism of a bacterial ZIP metal transporter. *Nature Communications 2023 14:1* **14**, 385. https://doi.org/10.1038/s41467-023-36048-4 (2023).
12. Bozzi, A. T. & Gaudet, R. Molecular mechanism of NRAMP-family transition metal transport. *J. Mol. Biol.* **433**, 166991. https://doi.org/10.1016/j.jmb.2021.166991 (2021).
13. Sun, B., Gu, L., Bao, L., Zhang, S., Wei, Y., Bai, Z., Zhuang, G., & Zhuang, X. Application of biofertilizer containing *Bacillus subtilis* reduced the nitrogen loss in agricultural soil. *Soil Biol. Biochem.* **148**, 107911. https://doi.org/10.1016/j.soilbio.2020.107911 (2020).
14. Ma, L., Terwilliger, A. & Maresso, A. W. Iron and zinc exploitation during bacterial pathogenesis. *Metallomics* **7**, 1541–54. https://doi.org/10.1039/c5mt00170f (2015).
15. Chu, L., Schäfer, C. C. & Matthes, M. S. Molecular mechanisms affected by boron deficiency in root and shoot meristems of plants. *J. Exp. Bot.* **76**, 1866–1878. https://doi.org/10.1093/jxb/eraf036 (2025).
16. Vera-Maldonado, P., Aquea, F., Reyes-Díaz, M., Cárcamo-Fincheira, P., Soto-Cerda, B., Nunes-Nesi, A., & Inostroza-Blancheteau, C. Role of boron and its interaction with other elements in plants. *Front. Plant Sci.* **15**, 1332459. https://doi.org/10.3389/fpls.2024.1332459 (2024).
17. Arif, H., Siraj, U., Ana, Ali, S., Zia, A., Ali, S., & De Lo Rios-Escalante, P. R. Synergistic roles of zinc and boron in enhancing growth, stress physiology, and heavy metal tolerance in *Brassica rapa* L. *Discover Plants* **3**, 21. https://doi.org/10.1007/s44372-026-00486-3 (2026).
18. Javed, A., Ahmad, A., Nouman, M., Hameed, A., Tahir, A., & Shabbir, U. Turnip (*Brassica rapus* L.): a natural health tonic. *Brazilian Journal of Food Technology* **22**. https://doi.org/10.1590/1981-6723.25318 (2019).
19. Glick, B. R. & Glick, B. R. Introduction to plant growth-promoting bacteria. *Beneficial plant-bacterial interactions* 1–37. https://doi.org/10.1007/978-3-030-44368-9 (2020).
20. Wimmer, M. A. & Eichert, T. Mechanisms for boron deficiency-mediated changes in plant water relations. *Plant Science* **203**, 25–32. https://doi.org/10.1016/j.plantsci.2012.12.012 (2013).
21. Wei, C., Jiao, Q., Agathokleous, E., Liu, H., Li, G., Zhang, J., & Jiang, Y. Hormetic effects of zinc on growth and antioxidant defense system of wheat plants. *Science of The Total Environment* **807**, 150992. https://doi.org/10.1016/j.scitotenv.2021.150992 (2022).
22. Shams, W. A., Siraj, U., Rehman, G., Ullah, Z., Ahmad, N., Miraj, M., & Khan, A. J. Physiochemical and Biological Properties of Water of Khyber Pakhtunkhwa District Bannu, Pakistan 2014. *International Journal of Photochemistry and Photobiology* **2**, 12–15. https://doi.org/10.11648/j.ijpp.20180201.13 (2018).
23. Siraj, U., Shams, W. A., Rehman, G. & Niaz, S. Serological Diagnosis of *Salmonella typhi* in DHQ (District Head Quarter Hospital) of Charsadda, City of Kp Pakistan. *Computational Biology and Bioinformatics* **6**, 21–24. https://doi.10.11648/j.cbb.20180601.12 (2018).
24. Mubeen, A., Saeed, M. T., Saleem, M. F. & Wahid, M. A. Zinc and Boron Application Improves Yield, Yield Components and Gross Returns of Mungbean (*Vigna radiata* L.). *Journal of Arable Crops and Marketing* **2**, 79–87. https://doi.org/10.33687/jacm.002.02.3521 (2020).
25. Gupta, R., Verma, N. & Tewari, R. K. Micronutrient deficiency-induced oxidative stress in plants. *Plant Cell Rep.* **43**, 213. https://doi.org/10.1007/s00299-024-03297-6 (2024).
26. Ali, M. M., Gull, S., Hu, X., Hou, Y. & Chen, F. Exogenously applied zinc improves sugar-acid profile of loquat (*Eriobotrya japonica* Lindl.) by regulating enzymatic activities and expression of their metabolism-related genes. *Plant Physiology and Biochemistry* **201**, 107829. https://doi.org/10.1016/j.plaphy.2023.107829 (2023).
27. Kaval, A., Yılmaz, H., Tunca Gedik, S., Yıldız Kutman, B. & Kutman, Ü. B. The Fungal Root Endophyte *Serendipita indica* (*Piriformospora indica*) Enhances Bread and Durum Wheat Performance under Boron Toxicity at Both Vegetative and Generative Stages of Development through Mechanisms Unrelated to Mineral Homeostasis. *Biology (Basel).* **12**, 1098. https://doi.org/10.3390/biology12081098 (2023).
28. Safdar, M. E., Qamar, R., Javed, A., Nadeem, M. A., Javeed, H. M. R., Farooq, S., & Ahmed, M. A Combined Application of Boron and Zinc Improves Seed and Oil Yields and Oil Quality of Oilseed Rape (*Brassica napus* L.). *Agronomy 2023, Vol. 13, Page 2020* **13**, 2020. https://doi.org/10.3390/agronomy13082020 (2023).
29. Effect of Irrigation Frequencies and Foliar Application of Zinc and Boron on Growth and Yield of Yellow Sarson (*Brassica rapa*). *Int. J. Plant Soil Sci.* **35**, 1355–1361. https://doi.org/10.9734/ijpss/2023/v35i203935 (2023).
30. Ahmad, M. A., Agha, B. S., Alabade, A. I., Ibraheem, F. F., Alalaf, A. H., Alalam, A. T. S., & Meftahizade, H. Synergistic effects of boron and zinc foliar applications on growth and post-harvest storage attributes of potato (*Solanum tuberosum* L.) cultivar Argana. *BMC Plant Biology 2025 25:1* **25**, 1623. https://doi.org/10.1186/s12870-025-07723-z (2025).

31. Nuraga, G. W., Feyissa, T., Demissew, S., Tesfaye, K. & Woldegiorgis, A. Z. Comparison of proximate, mineral and phytochemical composition of enset (*Ensete ventricosum* (Welw.) Cheesman) landraces used for a different purpose. *Afr. J. Agric. Res.* **14**, 1326–1334. https://doi.org/10.5897/AJAR2019.13993 (2019).
32. Punchay, K., Inta, A., Tiansawat, P., Balslev, H. & Wangpakapattanawong, P. Nutrient and mineral compositions of wild leafy vegetables of the Karen and Lawa communities in Thailand. *Foods* **9**, 1748. https://doi.org/10.3390/foods9121748 (2020).
33. Safdar, B., Pang, Z., Liu, X., Rashid, M. T. & Jatoi, M. A. Structural and functional properties of raw and defatted flaxseed flour and degradation of cynogenic contents using different processing methods. *J. Food Process Eng.* **43**, e13406. https://doi.org/10.1111/jfpe.13406 (2020).
34. Ali, H., Mahmood, I., Ali, M. F., Waheed, A., Jawad, H., Hussain, S., & Alamri, S. Individual and interactive effects of amino acid and paracetamol on growth, physiological, and biochemical aspects of *Brassica napus* L. under drought conditions. *Heliyon* **10**, 31544. https://doi.org/10.1016/j.heliyon.2024.e31544 (2024).
35. Xue, Y., Yan, W., Gao, Y., Zhang, H., Jiang, L., Qian, X., & Liu, K. Interaction Effects of Nitrogen Rates and Forms Combined With and Without Zinc Supply on Plant Growth and Nutrient Uptake in Maize Seedlings. *Front. Plant Sci.* **12**. https://doi.org/10.3389/fpls.2021.722752 (2021).
36. Farooq, H., Ishtiaq, R., Babar, H., Faryad, M. H., Ameen, M., Abbas, M. T., & Abdi, G. Enhancing zinc and iron biofortification in mungbean (*Vigna radiata* L.) through various application methods. *Scientific Reports 2025 15:1* **15**, 10974. https://doi.org/10.1038/s41598-025-95441-9 (2025).
37. Fan, X., Zhou, X., Chen, H., Tang, M. & Xie, X. Cross-Talks Between Macro- and Micronutrient Uptake and Signaling in Plants. *Front. Plant Sci.* **12**, 663477. https://doi.org/10.3389/fpls.2021.663477 (2021).
38. Shahrajabian, M. H., Kuang, Y., Cui, H., Fu, L., & Sun, W. Metabolic changes of active components of important medicinal plants on the basis of traditional Chinese medicine under different environmental stresses. *Curr. Org. Chem.* **27**, 782–806. https://doi.org/10.2174/1385272827666230807150910 (2023).
39. Gao, S., Tang, X., Zhang, J., Zhou, Q., Peng, T., Liu, A., & Li, P. Zinc-selenium interaction regulates leaf photosynthesis and mediates grain sugar metabolism to improve the yield and quality of hybrid rice: A physiological perspective. *Plant Physiology and Biochemistry* **221**, 109611. https://doi.org/10.1016/j.plaphy.2025.109611 (2025).
40. Malik, A. & Garg, V. K. *Bioremediation for Sustainable Environmental Cleanup*. https://doi.org/10.1201/9781003277941 (2024).
41. Kamran, A., Naveed, I., Jahan, S., Komal, L., Siddiqui, M. H., Alamri, S., & Khalil, A. Boron bioavailability enhanced by foliar applied fulvic acid to improve grain yield and quality of fine basmati rice. *Scientific Reports 2025 15:1* **15**, 30862. https://doi.org/10.1038/s41598-025-04747-1 (2025).
42. Mshanga, N., Moore, S., Kassim, N., Martin, H. D., Auma, C. I., & Gong, Y. Y. Association Between Aflatoxin Exposure and Haemoglobin, Zinc, and Vitamin A, C, and E Levels/Status: A Systematic Review. *Nutrients 2025, Vol. 17, Page 855* **17**, 855. https://doi.org/10.3390/nu17050855 (2025).
43. Jalil, S., Nazir, M. M., Ali, Q., Zulfiqar, F., Moosa, A., Altaf, M. A., & Jin, X. Zinc and nano zinc mediated alleviation of heavy metals and metalloids in plants: an overview. *Functional Plant Biology* **50**, 870–888. https://doi.org/10.1071/FP23021 (2023).
44. da Cristina Bungala, L. T., Van Nguyen, B., Park, C., Sathasivam, R., Bok, G., Park, J. S., & Park, S. U Analysis of Glucosinolates and Phenolic Content in Sprouts of 7 Brassica rapa Subspecies. *Nat. Prod. Commun.* **19**. https://doi.org/10.1177/1934578X2412585 (2024).
45. Zhang, X., Jia, Q., Jia, X., Li, J., Sun, X., Min, L., ... & Zhao, J. *Brassica* vegetables - an undervalued nutritional goldmine. *Hortic. Res.* **12**, https://doi.org/10.1093/hr/uhae302 (2025).
46. Serrano, C., Oliveira, M. C., Lopes, V. R., Soares, A., Molina, A. K., Paschoalinotto, B. H., & Barata, A. M. Chemical Profile and Biological Activities of Brassica rapa and *Brassica napus* Ex Situ Collection from Portugal. *Foods* **13**, 1164. https://doi.org/10.3390/foods13081164 (2024).
47. Dixon, R. A. & Paiva, N. L. Stress-Induced Phenylpropanoid Metabolism. *Plant Cell* **7**, 1085–1097. https://doi.org/10.1105/tpc.7.7.1085 (1995).
48. Alloway, B. J. Zinc in Soils and Crop Nutrition. *International Zinc Association and International Fertilizer Association* **16**, (2008).
49. Dai, Z., Huang, Z., Hu, D., Naz, M., Afzal, M. R., Raza, M. A., & Du, D. Role of Nanofertilization in Plant Nutrition under Abiotic Stress Conditions. *Chemosphere* 143496. https://doi.org/10.1016/j.chemosphere.2024.143496 (2024).
50. Bartolić, D., Baošić, R., Mutić, J., Stanković, M., Mutavdžić, D., Preradović, N., & Radotić, K. Associations Between Mineral Composition and Aflatoxin B1 in Maize (Zea mays L.) Seeds: Toward Contamination Indicators and Food Safety. *Foods* **14**, 3552. https://doi.org/10.3390/foods14203552 (2025).
51. Hu, P., Li, K., Peng, X., Yao, T., Zhu, C., Gu, H., & Cai, D. Zinc intake ameliorates intestinal morphology and oxidative stress of broiler chickens under heat stress. *Front. Immunol.* **14**, 1308907. https://doi.org/10.3389/fimmu.2023.1308907 (2024).
52. Qu, M., Huang, X., García-Caparrós, P., Shabala, L., Fuglsang, A. T., Yu, M., & Shabala, S. Understanding the role of boron in plant adaptation to soil salinity. *Physiol. Plant.* **176**, 14358. https://doi.org/10.1111/ppl.14358 (2024).
53. Pożarska, A., Karpiesiuk, K., Kozera, W., Czarnik, U., Dąbrowski, M., & Zielonka, Ł. AFB1 Toxicity in Human Food and Animal Feed Consumption: A Review of Experimental Treatments and Preventive Measures. *International Journal of Molecular Sciences 2024, Vol. 25, Page 5305* **25**, 5305. https://doi.org/10.3390/ijms25105305 (2024).
54. Karatekeli, S., Demirel, H. H., Zemheri-Navruz, F., & Ince, S. Boron exhibits hepatoprotective effect together with antioxidant, anti-inflammatory, and anti-apoptotic pathways in rats exposed to aflatoxin B1. *Journal of Trace Elements in Medicine and Biology* **77**, 127127. https://doi.org/10.1016/j.jtemb.2023.127127 (2023).
55. Safdar, M. E., Qamar, R., Javed, A., Nadeem, M. A., Javeed, H. M. R., Farooq, S., ... & Ahmed, M. A. Combined Application of Boron and Zinc Improves Seed and Oil Yields and Oil Quality of Oilseed Rape (*Brassica napus* L.). *Agronomy* **13**, 2020. https://doi.org/10.3390/agronomy13082020 (2023).
56. Ahmad, Z., Khaliq, A., Waraich, E. A., Artyszak, A., Zaman, Q. U., Abbasi, A., & Bamagoos, A. A. Exogenously Applied Silicon and Zinc Mitigate Salt Stress by Improving Leaf Pigments and Antioxidant Activities in Canola Cultivars. *Silicon* **15**, 5435–5444. https://doi.org/10.1007/s12633-023-02446-y (2023).
57. Bhadra, T., Mahapatra, C. K., Hosenuzzaman, M., Gupta, D. R., Hashem, A., Avila-Quezada, G. D., & Paul, S. K. Zinc and Boron Soil Applications Affect Athelia rolfsii Stress Response in Sugar Beet (*Beta vulgaris* L.) Plants. *Plants* **12**, 3509. https://doi.org/10.3390/plants12193509 (2023).
58. Kumari, V. V., Banerjee, P., Verma, V. C., Sukumaran, S., Chandran, M. A. S., Gopinath, K. A., & Awasthi, N. K. Plant Nutrition: An Effective Way to Alleviate Abiotic Stress in Agricultural Crops. *Int. J. Mol. Sci.* **23**, https://doi.org/10.3390/ijms23158519 (2022).
59. Pour-Aboughadareh, A., Khalili, M., Poczai, P. & Olivoto, T. Stability Indices to Deciphering the Genotype-by-Environment Interaction (GEI) Effect: An Applicable Review for Use in Plant Breeding Programs. *Plants (Basel).* **11**, https://doi.org/10.3390/plants11030414 (2022).
60. Halim, A., Paul, S. K., Sarkar, M. A. R., Rashid, M. H., Perveen, S., Mia, M. L., & Islam, A. M. Field Assessment of Two Micronutrients (Zinc and Boron) on the Seed Yield and Oil Content of Mustard. *Seeds* **2**, 127–137. https://doi.org/10.3390/seeds2010010 (2023).
61. Limcharoensuk, T., Chumsawat, W., Siraj, U., Krobthong, S., Pitchayawat, P., Hamkrasri, A., & Auesukaree, C. Aqueous extract of *Cissus quadrangularis* L. alleviates heavy metal toxicity in *Saccharomyces cerevisiae* by limiting metal uptake and enhancing detoxification mechanisms. *Ecotoxicol. Environ. Saf.* **299**, 1–13. https://doi.org/10.1016/j.ecoenv.2025.118408 (2025).
62. Ullah, A., Siraj, U., Muhammad, A., Junaid, M., Arif, H., Batool, S., & Ullah, S. Antimicrobial activity of *Parrotiopsis jacquemontiana* and *Caesalpinia decapetala* plant extracts against selected pathogens. *Natural and Applied Sciences International Journal (NASIJ)* **4**, 78–93. https://doi.org/10.47264/idea.nasij/4.2.5 (2023).
63. Wojtyla, Ł., Lechowska, K., Kubala, S. & Garnczarska, M. Different modes of hydrogen peroxide action during seed germination. *Front. Plant Sci.* **7**, 175649. https://doi.org/10.3389/fpls.2016.00066 (2016).
64. Awuchi, C. G., Ondari, E. N., Ogbonna, C. U., Upadhyay, A. K., Baran, K., Okpala, C. O. R., & Guiné, R. P. Mycotoxins Affecting Animals, Foods, Humans, and Plants: Types, Occurrence, Toxicities, Action Mechanisms, Prevention, and Detoxification Strategies—A Revisit. *Food* **10**, 1279. https://doi.org/10.3390/foods10061279 (2021).
65. Shin, C., Hwang, J. Y., Yoon, J. H., Kim, S. H., & Kang, G. J. Simultaneous determination of neurotoxic shellfish toxins (brevetoxins) in commercial shellfish by liquid chromatography tandem mass spectrometry. *Food Control* **91**, https://doi.org/10.1016/j.heliyon.2023.e21610 (2018).
66. AOAC. *Official Methods of Analysis of AOAC International.* (Association of Official Analytical Chemists, Gaithersburg, MD, 2005).
67. Shukla, S., Kumar, N., Bhardwaj, P., Verma, A., Patel, M. K., Rawat, M., & Saxena, S. Effect of farmyard manure and Azotobacter on the nutritional quality of high-altitude-grown cruciferous vegetables: an exploratory study. *J. Agric. Food Res.* **21**, 101947. https://doi.org/10.1016/j.jafr.2025.101947 (2025).
68. FAO/WHO. *Human Vitamin and Mineral Requirements: Report of a Joint FAO/WHO Expert Consultation*. (2003).
69. Shukla, S. *et al.* Effect of cold arid high-altitude environment on bioactive phytochemical compounds of organically grown Brassicaceae vegetables for nutri-health security in mountainous regions. *Sci. Rep.* **14**, 15976. https://doi.org/10.1038/s41598-024-64926-4 (2024).
70. Lamba, K., Kumar, M., Singh, V., Chaudhary, L., Sharma, R., Yashveer, S., & Dalal, M. S. Heat stress tolerance indices for identification of the heat-tolerant wheat genotypes. *Sci. Rep.* **13**, 10842. https://doi.org/10.1038/s41598-023-37634-8 (2023).

List of Abbreviations	
AAS	Atomic Absorption Spectrometry
AFB_1	Aflatoxin B1
APX	Ascorbate Peroxidase
AOAC	Association of Official Analytical Chemists
ACA	Acetyl-CoA Carboxylase
BOR	Boron-Requiring Efflux Transporter
B	Boron
CAT	Catalase
Cd	Cadmium
Cr	Chromium
DW	Dry weight
ELISA	Enzyme-Linked Immunosorbent Assay
FAO	Food and Agriculture Organization of the United Nations
Fe	Iron
FW	Fresh Weight
GAE	Gallic Acid Equivalents
GMP	Geometric Mean Productivity
GTs	Glycosyltransferases
HBV	Hepatitis B Virus
HCV	Hepatitis C Virus
HCC	Hepatocellular Carcinoma
HCN	Hydrogen Cyanide
IBGE	Institute of Biotechnology and Genetic Engineering
Mg kg^{-1}	Milligram per kilogram
µ kg^{-1}	Microgram per kilogram
Kcal 100 g^{-1}	Kilocalories per 100 grams
MTs	Mycotoxins
n	Number
Ni	Nickel
N	Nitrogen
NFE	Nitrogen-Free Extract
NIP	Noudlin-26-like Intrinsic Protein
NRAMP	Natural Resistance-Associated Macrophages Protein
PCA	Principal Component Analysis
Pb	Lead
Ppb	Parts per billion
POD	Peroxidase/Guaiacol Peroxidase
ROS	Reactive Oxygen Species
Rt-qPCR	Reverse Transcription Quantitative Polymerase Chain
RPI	Relative Performance Index
SOD	Superoxide Dismutase
STI	Stress Tolerance Index
TOL	Tolerance Index
SUT	Sucrose Transporter gene
WHO	World Health Organization
YSI	Yield Stability Index
ZIP	Zinc Regulated Transporter
Zn	Zinc